Primary and secondary relaxation process in plastically crystalline cyanocyclohexane studied by H-2 nuclear magnetic resonance. II. Quantitative analysis

ARTICLE *in* THE JOURNAL OF CHEMICAL PHYSICS · FEBRUARY 2013

Impact Factor: 2.95 · DOI: 10.1063/1.4790398 · Source: PubMed

3 AUTHORS:

Björn Micko
Landis+Gyr GmbH
7 PUBLICATIONS **53** CITATIONS
SEE PROFILE

Danuta Kruk
University of Warmia and Mazury in Olsztyn
73 PUBLICATIONS **845** CITATIONS
SEE PROFILE

Ernst Rössler
University of Bayreuth
205 PUBLICATIONS **5,493** CITATIONS
SEE PROFILE

Primary and secondary relaxation process in plastically crystalline cyanocyclohexane studied by 2H nuclear magnetic resonance. II. Quantitative analysis

B. Micko, D. Kruk, and E. A. Rössler

Citation: J. Chem. Phys. **138**, 074504 (2013); doi: 10.1063/1.4790398
View online: http://dx.doi.org/10.1063/1.4790398
View Table of Contents: http://jcp.aip.org/resource/1/JCPSA6/v138/i7
Published by the American Institute of Physics.

Primary and secondary relaxation process in plastically crystalline cyanocyclohexane studied by ^{2}H nuclear magnetic resonance. II. Quantitative analysis

B. Micko,[1] D. Kruk,[2] and E. A. Rössler[1,a)]
[1]*Experimentalphysik II, Universität Bayreuth, 95440 Bayreuth, Germany*
[2]*Faculty of Mathematics and Computer Science, University of Warmia and Mazury, PL-10710 Olsztyn, Poland*

(Received 17 September 2012; accepted 22 January 2013; published online 19 February 2013)

We analyze the results of our previously reported ^{2}H nuclear magnetic resonance (NMR) experiments in the plastically crystalline (PC) phase of cyanocyclohexane (Part I of this work) to study the fast secondary relaxation (or β-process) in detail. Both, the occurrence of an additional minimum in the spin-lattice relaxation T_1 and the pronounced effects arising in the solid-echo spectrum above the glass transition temperature $T_g = 134$ K, allow for a direct determination of the restricting geometry of the β-process in terms of the "wobbling-in-a-cone" model. Whereas at temperatures below T_g the reorientation is confined to rather small solid angles (below 10°), the spatial restriction decreases strongly with temperature above T_g, i.e., the distribution of cone angles shifts continuously towards higher values. The β-process in the PC phase of cyanocyclohexane proceeds via the same mechanism as found in structural glass formers. This is substantiated by demonstrating the very similar behavior (for $T < T_g$) of spin-lattice relaxation, stimulated echo decays, and spectral parameters when plotted as a function of $\langle \log \tau_\beta \rangle$ (taken from dielectric spectroscopy). We do, however, not observe a clear-cut relation between the relaxation strength of the β-process observed by NMR (calculated within the wobbling-in-a-cone model) and dielectric spectroscopy. © *2013 American Institute of Physics*. [http://dx.doi.org/10.1063/1.4790398]

I. INTRODUCTION

Glass forming substances of different molecular structure may exhibit a secondary relaxation, the β-process, which dominates the relaxation behavior below the glass transition temperature T_g.[1–10] Although the motion is highly hindered, the mechanism of motion was studied in detail by ^{2}H nuclear magnetic resonance (NMR) experiments in toluene,[11] for example, and successfully explained[12] via the model of a motion confined to the circumference of a cone ("cone-model"). It was demonstrated that essentially all molecules in the glass explore a rather small solid angle of below 10° due to the β-process, which proceeds via a complex sequence of small-angular reorientations.[13] This approach has proven to be applicable also for other glass forming systems.[14] Hence ^{2}H NMR detects a β-process of rather universal nature, whereas the relaxation strength in dielectric spectroscopy (DS) considerably varies among the systems.[10]

Above T_g the relaxation strength grows significantly, as documented by DS (cf. Figure 5(b)), i.e., within the cone model the spatial restriction is assumed to decrease, leading to a progressive correlation loss via the β-process. The process furthermore approaches the fast motion limit $\tau_\beta \ll 1/\delta$ (δ represents a measure of the ^{2}H NMR interaction strength and is typically on the order of 130 kHz) in this temperature range, hence in principle pronounced effects in the NMR observables are anticipated. Yet the β-process is commonly not accessible to ^{2}H NMR methods in the supercooled regime ($T > T_g$) as the time scales of the structural relaxation, the α-process, and the β-process typically merge slightly above T_g. This does, however, not hold in all systems: in Part I of this work[15] we presented a ^{2}H NMR study of the relaxation processes in the (supercooled) plastically crystalline (PC) phase of cyanocyclohexane (CNCH), which exhibits a β-process (cf. Figure 1) that is very similar to the β-process in structural glass formers at $T < T_g$. Above T_g however the time scales of α- and β-process in CNCH are well separated even at the highest temperatures and $\tau_\beta \ll 1/\delta$ holds for virtually all sub-ensembles. Hence, we were able to study the effects of the β-process well above T_g and observed pronounced line-shape effects in a broad temperature range and an additional minimum in the spin-lattice relaxation T_1 associated with the β-process. Regarding the α-process, we have demonstrated that the motion is not governed by the translational symmetry of the PC lattice: in contrast to other PC systems like cyanoadamantane[16] the mode of reorientation in CNCH is very similar to the one observed in structural glass formers,[17] i.e., can be modeled via a distribution of small and large angular jump processes by which the orientation of a molecule explores the full unit sphere in the course of time – in other words: the motion is "liquid-like."

The scope of the present contribution is to quantitatively exploit the features in the spin-lattice relaxation T_1 and the solid-echo line-shape with regard to the fast β-process in CNCH. A detailed analysis of T_1 allows for an extraction of the relaxation strength of the β-process, $1\text{-}f^{(l)}$, over the whole

a)Author to whom correspondence should be addressed. Electronic mail: ernst.roessler@uni-bayreuth.de.

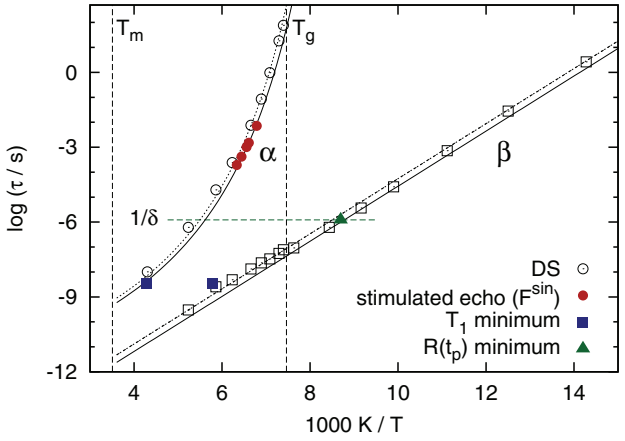

FIG. 1. Correlation times of the α- and β-process in the PC phase of CNCH, ^{2}H NMR results from Part I,[15] dielectric time constants from Ref. 18. The dotted lines represent fits to the dielectric time constants, the full lines are the interpolations employed in the calculation of T_1, as our previous ^{2}H NMR results appear slightly shifted in temperature with respect to dielectric data (we found $\tau_\beta(T) = 2.5 \times 10^{-16} \exp(2542\ \mathrm{K}/T)$ and $\tau_\alpha(T) = 1.5 \times 10^{-12} \exp(1064\ \mathrm{K}/(T - 100\ \mathrm{K}))$). The horizontal dotted line marks $\tau = 1/\delta$, i.e., discriminates between ^{2}H NMR fast- and slow-motion regime.

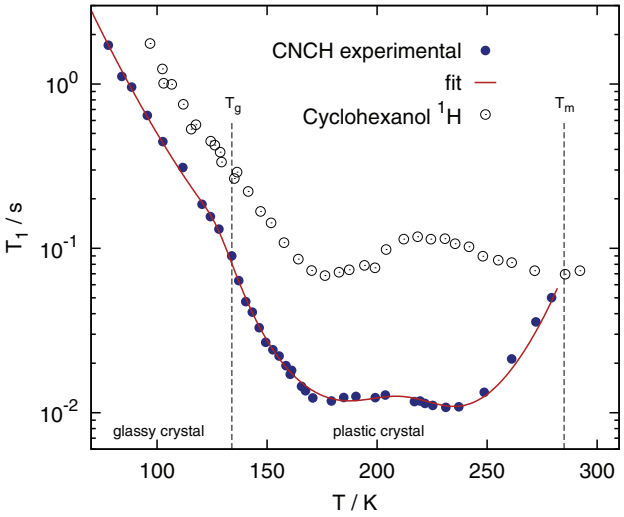

FIG. 2. Average spin-lattice relaxation times $\langle 1/T_1 \rangle^{-1}$ of CNCH (full symbols) and corresponding fit via Eq. (7) (solid red line). Included for comparison is the ^{1}H T_1 data of cyclohexanol[26] recorded at $\omega_L = 2\pi \times 21$ MHz, the indicated T_g and T_m correspond to CNCN.

accessible temperature range with $f^{(l)}$ being defined by

$$\lim_{t\to\infty} F^{(l)}(t) = f^{(l)}; \quad T < T_g, \tag{1}$$

where $F^{(l)}$ represents the rank l reorientational correlation function and $f^{(l)}$ denotes the relaxation strength of the α-process at $T > T_g$. The fast motion limit line-shape ($\tau_\beta \ll 1/\delta$) at $T > T_g$ furthermore allows us to directly determine the restricting geometry of the process in terms of a distribution of cone angles $G(\chi; T)$, from which again 1-$f^{(l)}$ can be obtained (for $l = 1, 2$). Finally, we will compare the results of both ^{2}H NMR techniques with the dielectric relaxation strength (assumed to be) given by $1 - f^{(1)} = \Delta\epsilon_\beta/\Delta\epsilon$.

As we will demonstrate, the two ^{2}H NMR techniques provide consistent relaxation strengths 1-$f^{(2)}$, whereas we cannot rationalize the corresponding quantity 1-$f^{(1)}$ from DS. Moreover, the present NMR findings are very similar when compared to results reported for structural glasses, while the relaxation strength of the corresponding dielectric spectra significantly varies. In particular, we substantiate the first conclusion by comparing additional results from stimulated echo experiments as well as spin-lattice relaxation T_1 in CNCH with some structural glass formers. As in the case of depolarized light scattering ($l = 2$), which does not detect the β-process at all,[19–21] it is difficult to explain the relaxation strength observed in DS within the single-particle dynamics revealed by NMR.

II. RESULTS

A. Modeling the spin-lattice relaxation T_1

Figure 2 displays the spin-lattice relaxation times $\langle 1/T_1 \rangle^{-1}$ (obtained from the initial decay of the magnetization curves) of CNCH, which were qualitatively discussed in Part I.[15] Two pronounced minima between T_g and T_m, corresponding to α- and β-process, are resolved. For a quantitative analysis, we model T_1 in the PC phase (i.e., below $T_m = 285$ K) within a model-free approach in which the orientational correlation function F_2 decays to a plateau value $f^{(2)}$ due to the β-process, whereas the isotropic tumbling motion of the α-process destroys any remaining correlation at later times. Due to the fast β-process in CNCH the assumption of time scale separation is valid at all temperatures and the total susceptibility can be obtain from an additive ansatz

$$\chi''^{(l)}(\omega) = f^{(l)}\chi''_\alpha(\omega) + (1 - f^{(l)})\chi''_\beta(\omega), \tag{2}$$

which resembles the Williams-Watts[6] approach in dielectric spectroscopy as well as the model independent approach by Lipari and Szabo in NMR[22] and allows us to extract the relaxation strength 1-$f^{(2)}$ or square of the generalized order parameter $\mathcal{S}^2 = f^{(2)}$ of the β-process.

Under the assumption that the relaxation strength $f^{(l)}$ is probe dependent but the individual susceptibilities $\chi''_{\alpha/\beta}$ are not (regarding the α-process this approximation has proven to be valid[21,23]), we can employ the imaginary part of the normalized, complex susceptibilities applied by Tschirwitz *et al.*[18] to interpolate the dielectric spectra in Eq. (2): a Cole-Davidson function for the α-process and a log-Gaussian susceptibility of width $\mathcal{W}$ for the β-process

$$\begin{aligned} \chi''_\alpha(\omega) &= \mathrm{Im}\left\{\frac{1}{\left(1 + i\omega\tau_\alpha^{\mathrm{CD}}\right)^{\beta_{\mathrm{CD}}}}\right\}, \\ \chi''_\beta(\omega) &= \frac{\sqrt{\pi}}{2\mathcal{W}\ln 10}\exp\left[-\frac{log^2\left(\frac{\omega\tau_\beta}{2\pi}\right)}{\mathcal{W}^2}\right]. \end{aligned} \tag{3}$$

We will adopt this description for our T_1 analysis, as the corresponding shape parameters are readily available in Ref. 18. Hence, we are able to calculate the individual susceptibilities employing the time constants τ_α, τ_β and shape parameters $\mathcal{W}$, β_{CD} from dielectric spectroscopy. As we observed, a slight deviation in the time constants reported from DS[18]

with respect to our ^{2}H NMR results, the interpolations given by the full lines in Figure 1 were employed in the calculation (the parameters are given in the key of Figure 1, the fits to the dielectric results are represented by the dashed lines). The stretching parameter β_{CD} of the α-process was interpolated from the results given in Ref. 18. The width parameter $\mathcal{W}$ of the β-process was obtained from the DS experiments[18] and follows:

$$\mathcal{W} = \frac{\sigma}{k_B \ln 10} \cdot \left(\frac{1}{T} - \frac{1}{T_\delta} \right), \tag{4}$$

(with the constants $\sigma = 1162\,\mathrm{K}\,k_B$ and $T_\delta = 440\,\mathrm{K}$) above as well as below T_g in good approximation.

The spectral densities $J^{(2)}_{\alpha/\beta}(\omega)$ are subsequently calculated from the normalized susceptibilities via the fluctuation dissipation theorem[24]

$$J^{(2)}_{\alpha/\beta}(\omega) = \frac{\chi''^{(2)}_{\alpha/\beta}(\omega)}{\omega}, \tag{5}$$

and the total spectral density $J^{(2)}(\omega)$ is obtained analogous to Eq. (2),

$$J^{(2)}(\omega) = f^{(2)} J_\alpha(\omega) + (1 - f^{(2)}) J_\beta(\omega), \tag{6}$$

whereby the presumably l-dependent relaxation strength 1-$f^{(2)}$ serves as the only fit-parameter, as all other time scale and shape parameters are obtained from dielectric and our previous NMR results. To reproduce the experimentally observed T_1 values, 1-$f^{(2)}$ was modeled via a phenomenological function which qualitatively mimics the behavior observed in dielectric spectroscopy: weak, almost linear temperature dependence below T_g, around which 1-$f^{(2)}$ changes its slope and rises steeply towards higher temperatures.

In a final step T_1 is then obtained via[25]

$$\left\langle \frac{1}{T_1} \right\rangle = \frac{2}{15} \delta^2 [J^{(2)}(\omega_L) + 4J^{(2)}(2\omega_L)] \tag{7}$$

with the Larmor frequency $\omega_L = 2\pi \times 46.07$ MHz. The coupling constant δ was taken from the solid-echo spectrum at low temperatures, where the line shape becomes independent of temperature (we determined $\delta = 2\pi \times 129.6$ kHz from the spectrum recorded at $T = 34$ K, cf. the inset in Figure 6).

We have to remind, however, that T_1 in a solid depends on the orientation of the electric field gradient tensor with respect to the external magnetic field and hence Eq. (7) does not strictly hold.[27] The non-exponential character of the spin-lattice relaxation arising from this effect in the powder-averaged quantities is, however, small with regard to the non-exponentiality caused by the pronounced dynamic heterogeneities found in disordered systems ($T \lesssim T_g$). As the resulting stretched exponential magnetization curves are furthermore affected by spin diffusion at low temperatures, we have to consider $\langle 1/T_1 \rangle^{-1}$ determined from the initial slope in the experiment. In this quantity, the effects arising from the orientation dependence in T_1 can be accounted for via a rescaled coupling constant[28,29] δ^{eff} which yields a factor on the order of one. Since we employ the coupling constant obtained from the solid-echo spectra at low temperatures in our analysis ($\delta^{\mathrm{eff}} = \delta(34\mathrm{K}) = 2\pi \times 129.6$ kHz), any error due to the anisotropy of T_1 is included in the fitting parameter 1-$f^{(2)}$ (cf. below).

The solid line in Figure 2 is calculated in the described manner and demonstrates excellent agreement with experimental results over the whole accessible temperature range: $\langle 1/T_1 \rangle^{-1}$ below as well as above T_g – including the two minima – is fully reproduced. The temperature dependence of the relaxation strength 1-$f^{(2)}$ is displayed in Figure 5(b) (full line) and is roughly proportional to the dielectric results. However, the absolute relaxation strengths of the β-process obtained via ^{2}H NMR spin-lattice relaxation measurements (rank $l = 2$ correlation function) and dielectric spectroscopy ($l = 1$) cannot be compared in a model free approach. In the limit of small-angular motion a factor of three in 1-$f^{(l)}$ is anticipated between the different techniques[21,23,30]

$$1 - f^{(1)} = \frac{1}{3}[1 - f^{(2)}]. \tag{8}$$

Instead of a ratio three, however, one finds a factor of ≈6 at low temperatures in Figure 5(b). As discussed, the results of the present analysis may contain a systematic deviation resulting from the effective, reduced coupling constant for anisotropic motion, which is mapped to 1-$f^{(2)}$ in our approach. The expected deviations arising from this effect are, however, much smaller. Hence the (inherent) discrepancy between ^{2}H NMR and dielectric results will be discussed in a more general framework in Sec. II C.

Nevertheless the present analysis demonstrates that the individual spectral densities $J^{(1)}_{\alpha/\beta}(\omega, T)$ from dielectric spectroscopy are sufficient to fully describe the experimentally observed spin-lattice relaxation times at all temperatures; therefore, accordance between techniques probing $l = 1$ and $l = 2$ is found (with the exception of 1-$f^{(l)}$). The extracted relaxation strength 1-$f^{(2)}$ follows the same temperature trend as 1-$f^{(1)}$ obtained by DS. The T_1 analysis allows to extract the relaxation strength also at much higher temperatures than accessible to DS: strikingly no plateau is observed in 1-$f^{(2)}$ even at highest temperatures close to T_m. To model the experimental $\langle 1/T_1 \rangle$, a steady growth of the relaxation strength is needed. At the temperature of the T_1 minimum for the α-process, 1-$f^{(2)}$ is already about 0.7−0.8, hence it appears as if the β-process dominates the relaxation behavior in the PC phase at high temperatures.

B. Modeling the solid-echo spectra

In Part I,[15] we have discussed the peculiar solid-echo line-shape changes of CNCH at temperatures above T_g = 134 K, cf. Figures 3 and 4. The pronounced deviation from a Pake pattern arises due to the fast motion of the β-process and in the following allows to determine its restricting geometry. In other words: as α- and β-process are well separated in CNCH, a broad temperature interval above T_g opens where pre-averaging effects caused by the spatially hindered β-process can be observed in the NMR spectra before the α-process leads to a full collapse of the spectrum at higher temperatures.

As the simple cone model was successful in the description of the t_p-dependent line shape effects below T_g in

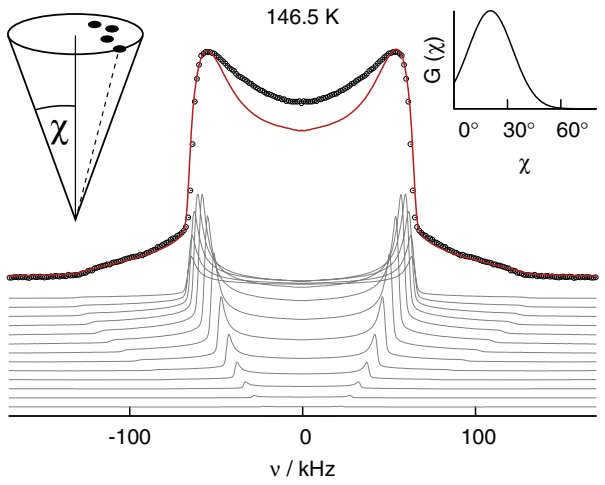

FIG. 3. Solid-echo spectrum at 146.5 K (open symbols), simulation (solid red line) within the wobbling-in-a-cone model (cf. Eq. (9) and the above sketch) and comprising sub-spectra of different $\bar{\delta}(\chi)$ (grey lines). A step size of 5° was chosen in χ for the displayed sub-spectra, the simulated spectrum consists of sub-spectra with a step-size of 1° however. The right inset displays the corresponding distribution of cone opening angles $G(\chi; T)$.

previous studies of the β-process,[13] it will also be employed in the present analysis at $T > T_g$. Due to the relatively low activation energy of the β-process in CNCH (with respect to T_g), the better part of the distribution $G_\beta(\log\tau)$ exhibits correlation times in the limit $\tau_\beta \ll 1/\delta$ at temperatures $T > T_g$. This situation is quite favorable for the present analysis, as the details of the dynamic process, i.e., the elementary jump angles γ and possible correlations of the jump time τ_j, γ, and the restriction χ, have no influence on the line shape in this limit any more. All models based on the geometrical restriction to a cone, therefore, differ only by the distribution of angles Θ, that are accessible after an infinite number of jumps. Consequently, we will only consider the limiting case of a wobbling motion within a cone[31–33] of half opening angle χ, where a C−^{2}H bond freely diffuses on the unit sphere within a cone and which yields a Pake spectrum of reduced apparent coupling constant $\bar{\delta}$ in the limit $\tau \ll 1/\delta$,[34]

$$\bar{\delta} = \delta\frac{1}{2}\cos(\chi)\left[1+\cos(\chi)\right]. \tag{9}$$

For a given cone angle χ, the resulting powder spectrum is hence expected to be merely reduced in width. Regarding the peculiar line-shape of CNCH in the temperature range under discussion (cf. open symbols in Figure 3), it is evident that the experimentally observed spectra cannot be described via a fixed opening angle χ, as they – apart from the overall narrowing – exhibit a significant broadening of the singularities, which can only be reproduced in the scope of the proposed model via a distribution of cone angles $G(\chi; T)$. As such a distribution was previously found in the analysis of the t_p-dependent ^{2}H NMR line-shape of, e.g., toluene,[12] it appears justified not only to take into account a distribution of correlation times $G_\beta(\log\tau)$, but also to assume a distribution of restricting geometries. This approach can however only be applied as long as $\tau_\beta \ll \tau_\alpha$, i.e., the isotropic motion of the α-process does not yield exchange between the different sub-ensembles. In CNCH, this condition is fulfilled at temperatures $T \leq 150$ K.[15]

As not all sub-ensembles of $G_\beta(\log\tau)$ are found in the fast motion limit $\tau_\beta \ll 1/\delta$ at all temperatures above T_g, the spectra are composed of a pre-averaged part S_{fast} and a rigid limit spectrum S_{slow},

$$S(\omega; T) = [1 - W(T)]\, S_{\text{fast}}(\omega; T) + W(T) S_{\text{slow}}(\omega), \tag{10}$$

whereby the weighting factor $W(T)$ is determined from the distribution of correlation times $G_\beta(\log\tau)$,

$$W(T) = \int_{\log 1/\delta}^{\infty} G_\beta(\log\tau, T)\, d\log\tau, \tag{11}$$

observed in dielectric spectroscopy[18]

$$G_\beta(\log\tau) = N_2(a,b)\left[b\left(\frac{\tau}{\tau_\beta}\right)^a + \left(\frac{\tau}{\tau_\beta}\right)^{-ab}\right]^{-1}. \tag{12}$$

N_2 represents a normalization factor and the shape parameters a, b in Eq. (12) control the symmetric/asymmetric broadening of the peak, respectively. According to the results of DS[18] the shape parameter b was set to one (symmetric distribution) and a was interpolated according to $a(T) = [0.6626(1000\text{ K}/T - 2.27)]^{-1}$. The pre-averaged line-shape S_{fast} is constructed

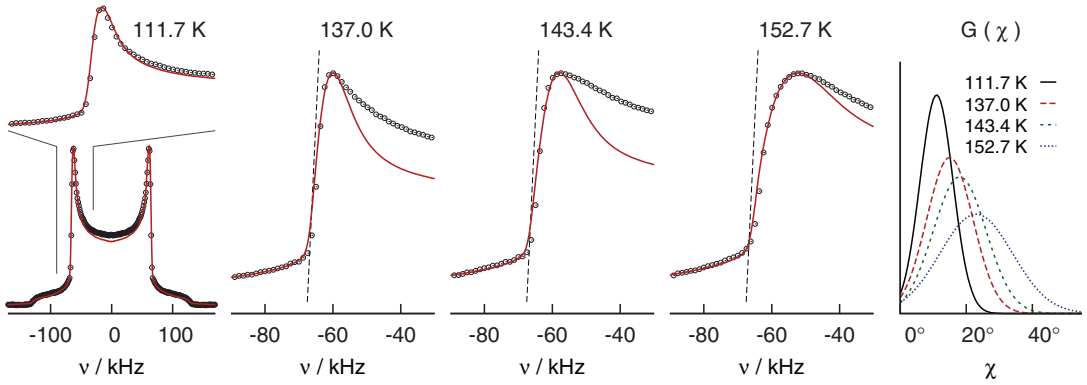

FIG. 4. Solid-echo spectra for short inter-pulse delays $t_p = 20\ \mu$s (open symbols) at different temperatures with according simulations (solid red lines) within the wobbling-in-a-cone model ($T_g = 134$ K). All experimental spectra have been symmetrized and for the higher temperatures only a blow-up around the lower, inner singularity is displayed. The dashed lines indicate the position and slope of the singularity in the spectrum at lowest temperatures, $T = 34$ K. The rightmost plot displays the corresponding distributions of cone opening angles $G(\chi; T)$.

from a weighted sum of Pake spectra with reduced apparent spectral widths $\bar{\delta}$, reflecting different cone angles χ,

$$S_{\text{fast}}(\omega;T) = \sum_{\chi=0^\circ}^{90^\circ} G(\chi;T)\, s(\omega;\bar{\delta}(\chi)). \tag{13}$$

For $S_{\text{slow}}(\omega) = s(\omega;\delta_0)$ in Eq. (10), we employed again the experimental spectrum recorded at the lowest temperature (34 K). The sub-spectra $s\left(\omega;\bar{\delta}(\chi)\right)$ were adapted from $s(\omega;\delta_0)$ via a rescaling of the frequency axis along Eq. (9). As pulse-lengths and damping were kept constant at all temperatures, this procedure yields less potential systematic error than the application of a numerically calculated Pake spectrum. The experimental spectra have been symmetrized to reduce the number of free parameters otherwise needed if small asymmetries arise due to slight impedance mismatching (for the original data see Paper I[15]).

We find that a simple Gaussian distribution of cone angles $G(\chi;T)$ proves to be versatile enough to fully reproduce the line-shape around the singularities in CNCH at temperatures above T_g and for short inter-pulse delays t_p,

$$G(\chi;T) = \frac{1}{\sqrt{2\pi}\sigma(T)} e^{-\frac{(\chi-\chi_\mu(T))^2}{2\sigma^2(T)}}. \tag{14}$$

The calculated spectrum $S(\omega;T)$ represented by the solid red line in Figure 3 is obtained in this manner (the corresponding distribution $G(\chi;T)$ is given in the inset): the line shape around the inner and outer singularities is fully reproduced via the fit, while deviations arise around zero frequency. The latter are possibly caused by the assumption of a symmetric distribution $G(\chi)$ or by the α-process, which exhibits a rather pronounced stretching in CNCH, and may render the solid-echo line-shape t_p-dependent in the discussed temperature regime (cf. Part I[15]). Yet the α-process is however too slow to affect the line shape around the singularities at the studied temperatures: the observed pronounced pre-averaging effects can only be attributed to the β-process below 160 K−165 K, where the line shape changes with temperature are subtle over a range of 35 K, whereas the α-process surpasses the time window of the experiment within 5 K at higher T. Consequently, the fits were conducted for spectra with the shortest inter-pulse delays t_p (20 μs) and the intensity in the center was neglected.

Figure 4 demonstrates the quality of the fits achieved in the described manner for different temperatures: the singularities of all spectra are fully reproduced within the experimental error via a temperature dependent distribution $G(\chi;T)$. Due to the pronounced reduction in the spectral width and the broadening of the singularities with increasing temperature, a stable fit could be obtained while neglecting the intensity in the central part. Hence, we are able to obtain the restricting geometry of the β-process directly at all temperatures from the solid-echo line-shape.

The parameters of $G(\chi;T)$, i.e., the most probable cone opening angle χ^m (cf. Eq. (14): as angles $\chi < 0$ do not appear in $G(\chi;T)$, we plot χ^m instead of χ_μ) and the standard deviation σ obtained from each experimental spectrum at temperatures 100 K $< T <$ 170 K are displayed in Figure 5(a): at temperatures below T_g, the distribution is centered around $\chi^m \approx 11^\circ$ and rather narrow, which is in fair agreement with

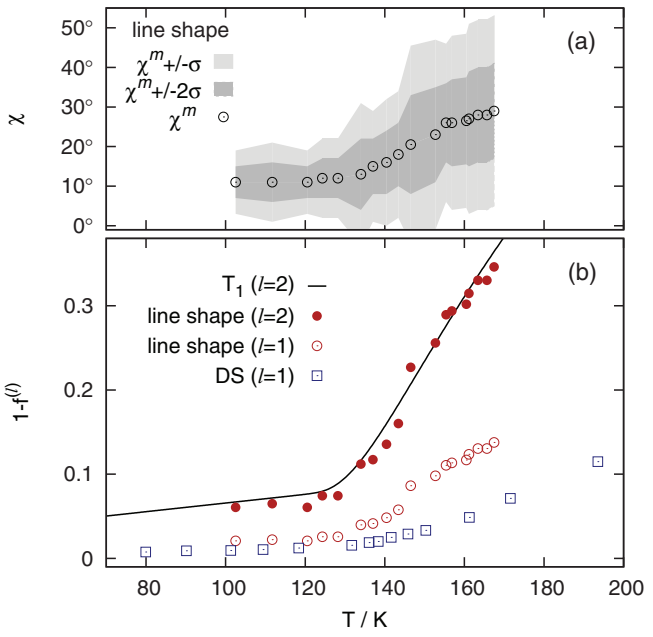

FIG. 5. (a) Parameters of the Gaussian distribution of opening angles $G(\chi;T)$ used to model the fast motion limit effect on the solid-echo spectra for $t_p = 20$ μs within the wobbling-in-a-cone model. (b) Corresponding relaxation strength 1-$f^{(l)}$ according to Eq. (18) in comparison with results from the T_1-analysis and dielectric spectroscopy.[18]

previous results.[12] Above T_g the most probable cone angle grows strongly – i.e., the temperature dependence of χ^m qualitatively resembles the one of the relaxation strength 1-$f^{(l)}$ obtained by DS and from the T_1 analysis in Sec. II A. Furthermore, the distribution $G(\chi;T)$ significantly broadens in this region.

1. Extension towards $T < T_g$

Whereas the described fitting procedure works well at temperatures $T > T_g$, where the fast motion limit effects are articulate, a determination of $G(\chi;T)$ becomes difficult at temperatures $T <$ 120 K as the line-shape for $t_p = 20$ μs closely resembles the rigid limit Pake spectrum. Nevertheless even below T_g a fraction of molecules exists with $\tau_\beta \ll 1/\delta$, i.e., sub-ensembles are found in the fast motion limit even at lowest temperatures and one expects subtle spectral changes for $t_p \to 0$ also below T_g (aside from the t_p-dependence of the solid-echo line shape discussed in Part I[15]).

The inset in Figure 6 displays the (symmetrized) spectrum at low temperatures (34.5 K), where the line-shape is well described by a Pake spectrum, as demonstrated by the fit symbolized by the solid line. Also marked in this figure are the measures C_x, defined as the apparent spectral widths at $x = 50\%$, 80%, and 100% of maximum intensity which will serve to quantify the spectral evolution at higher temperatures, as even below T_g the spectra no longer can be described by a Pake pattern.

In Figure 6, the shape parameters C_x are displayed for all recorded solid-echo spectra ($t_p = 20$ μs, cf. Part I[15]) at $T <$ 160 K. It becomes obvious that the spectral shape changes with temperature also below T_g. Whereas the apparent spectral widths C_x exhibit almost no temperature dependence at

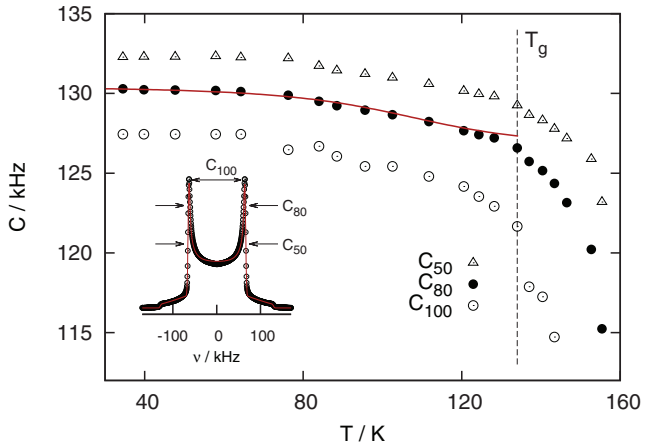

FIG. 6. Apparent spectral widths C_x of CNCH in the low temperature regime. The quantities C_x are defined via the inset (open symbols: experimental spectrum at $T = 34.5$ K, full red line: fit via a numerically calculated Pake spectrum, $\delta = 2\pi \times 129.6$ kHz). The red line corresponding to C_{80} results from a calculation via Eq. (15).

low temperatures, they start to lessen around $T = 60$ K and decrease approximately linear until T_g. At T_g the temperature dependence changes due to the stronger pre-averaging caused by the growing relaxation strength and the C_x values drop with temperature until the solid state spectrum finally vanishes due to the isotropic averaging of the quadrupolar coupling by the α-process ($T > 165$ K).

As the relaxation strength (and consequently the distribution $G(\chi; T)$) of the β-process is virtually constant below T_g, we can test the predictions of our present model at $T < T_g$ by setting a fixed, temperature independent distribution $G(\chi)$ obtained at an arbitrary temperature below T_g. As the distribution $G(\chi)$ furthermore becomes rather narrow below T_g, we can approximate the line shape changes via the most probable cone angle $\chi^m \approx 11^\circ$ found in this region and calculate the spectra directly via a modification of Eq. (10),

$$S(\omega; T < T_g) = [1 - W(T)]\, s(\omega; \bar{\delta}(\chi^m)) + W(T) s(\omega; \delta_0). \tag{15}$$

This allows us to compare the apparent spectral widths C_x of $S(\omega, T < T_g)$ with the experimentally obtained values. The full red line in Figure 6 was calculated for C_{80} in this manner. The temperature dependence of C_{80} is fully reproduced until close to T_g, where $1\text{-}f^{(l)}$ starts to grow and hence a temperature independent distribution $G(\chi)$ is no longer justified. Hence, we have demonstrated that all line shape changes (for $t_p = 20$ μs) in the region 34 K$\leq T <$165 K are consistently captured by the wobbling-in-a-cone model.

2. Comparison of results: $1\text{-}f^{(l)}$

In order to compare the ^{2}H NMR results from the lineshape and T_1 analysis, respectively, the relaxation strength of the β-process, $1\text{-}f^{(l)}$, is calculated from $G(\chi; T)$. In a second step, we then compare the NMR relaxation strength with the values reported by DS. The relaxation strength $1\text{-}f^{(l)}$ can be obtained directly from $G(\chi; T)$ via the average distribution of reorientation angles Θ with respect to the initial orientation, $g(\Theta)$. For a fixed cone opening angle χ, $f^{(l)}$ is given via[23]

$$f_\chi^{(l)} = \int g(\Theta; \chi)\, P_l(\cos\Theta)\, d\Theta, \tag{16}$$

where P_l denotes the Legendre polynomial of rank l. For the present wobbling-in-a-cone model, the resulting relaxation strength for a given cone angle χ reads[22,31,32]

$$f_\chi^{(l)} = \begin{cases} \frac{1}{4}(1+\cos\chi)^2, & \text{for } l = 1 \\ \frac{1}{4}\cos^2\chi\,(1+\cos\chi)^2, & \text{for } l = 2. \end{cases} \tag{17}$$

The relaxation strength corresponding to a given fit is then obtained in the same manner as the spectrum itself, i.e., via the distribution $G(\chi; T)$,

$$f^{(l)}(T) = \int_0^{\pi/2} G(\chi; T)\, f_\chi^{(l)} d\chi. \tag{18}$$

The resulting relaxation strengths $1\text{-}f^{(l)}$ for ranks $l = 1, 2$ are plotted in Figure 5(b). The relaxation strength $1\text{-}f^{(2)}$ (full circles) reproduces the values found by means of the spin-lattice relaxation model (solid line) rather well, i.e., the quantitative analysis of our NMR results is consistent: the geometries $G(\chi; T)$ extracted from the solid-echo line shape are in full agreement with the T_1-analysis.

With respect to dielectric results ($l = 1$, cf. open circles in Figure 5(b)); however, a clear deviation is found, as already anticipated from the T_1 analysis, where a difference between ranks $l = 1$, 2 larger than a factor of three was observed. The possible nature of this discrepancy will be discussed in Sec. II C. As the NMR results are consistent and the extracted relaxation strength is proportional to the dielectric results, we can conclude at this point that the assignment of the peculiar solid-echo line shape above T_g to the β-process is valid and that the employed model appears applicable to describe its restricting geometry.

C. Stimulated echo measurements and the universal manifestation of the β-process in NMR

Before discussing the differences between the NMR and DS results, we want to stress once again the similarities concerning the manifestation of the β-process in the PC phase of CNCH, in the structural glass formers toluene and ethanol and in a binary glass mixture of chlorobenzene and decalin at temperatures $T < T_g$.

For a comparison regarding the mechanism of motion and spatial restriction of the β-process, t_e-dependent stimulated echo measurements below T_g were conducted in CNCH, corresponding data for toluene and ethanol is available in Refs. 11 and 13. Figure 7(a) displays the decay curves of the cosine-cosine correlation function $F^{cos}(t_e; t_m)$ (corrected for T_1 relaxation effects during t_m, cf. Part I for details) for three different evolution times t_e at $T < T_g$: for an evolution time of 3 μs toluene (open symbols) exhibits a very weak decay until about $t_m = 100$ ms, when another process damps the stimulated echo amplitude to zero, which was attributed to spin diffusion effects.[11] For longer evolution times (30 μs and 80 μs), the initial decay grows in amplitude. As the decay extends over several orders of magnitude in time and is almost

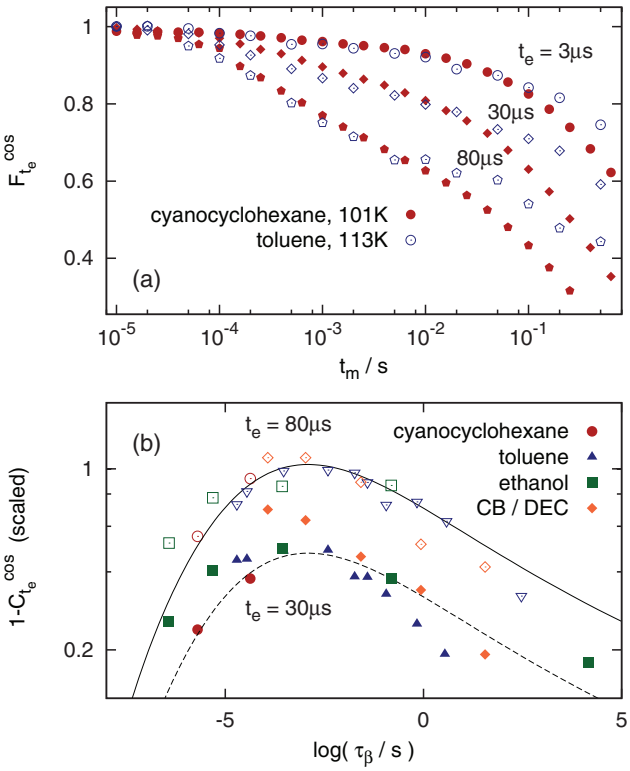

FIG. 7. (a) Stimulated echo decays of the cosine-cosine correlation in CNCH (full red symbols) and toluene (open black symbols, adapted from Ref. 11) for different evolution times t_e at temperatures $T < T_g$. (b) Scaled amplitude of the initial $F^{cos}(t_e; t_m)$ decay in CNCH, toluene[11] and ethanol[35] on an isodynamic temperature scale with respect to the β-process. The lines represent $p(t_e)A(T)$ (cf. Eq. (21)) calculated for CNCH from dielectric results.[18]

not observed for short evolution times, it has to be attributed to a highly restricted process with a broad distribution of correlation times: the β-process.

Stimulated echo decays of CNCH at a temperature chosen to reflect comparable τ_β are included in Figure 7(a): the initial decay is very similar to the case of toluene, especially with regard to the evolution time dependence. Significant differences arise only at longer mixing times t_m, when $F^{cos}(t_e; t_m)$ is dominated by spin diffusion effects, as the magnitude of the latter may differ among the systems.

Following the analysis in Ref. 11, the stimulated echo curves were fitted with a phenomenological function:

$$F^{cos}_{t_e}(t_m) = A_0\left[\left(1 - C^{cos}_{t_e}\right)\Phi_{\beta,t_e}(t_m) + C^{cos}_{t_e}\right]\Phi_{SD,t_e}(t_m), \tag{19}$$

where $\Phi_{\beta,t_e}(t_m)$ and $\Phi_{SD,t_e}(t_m)$ denote stretched exponential functions, reflecting the initial decay due to reorientation (β-process) and the long-time decay due to spin diffusion. As the relaxation strength of the β-process is nearly constant below T_g, the amplitude $1 - C^{cos}_{t_e}$ can be decomposed (in a scenario of heterogeneous dynamics) via[11]

$$1 - C^{cos}_{t_e} = p(t_e)\,A(T). \tag{20}$$

The quantity $A(T)$ accounts for the fraction of molecules within the experimental time window (from ≈100 μs due to experimental constraints to the onset of spin diffusion at around 100 ms) at a given temperature

$$A(T) = \int_{\log 100\mu s}^{\log 100ms} G_\beta(\log\tau, T)\, d\log\tau, \tag{21}$$

whereby the distributions $G_\beta(\log\tau)$ are obtained from dielectric spectroscopy and $p(t_e)$ represents a geometrical factor that accounts for the evolution time dependence, i.e., is sensitive on the elementary angular step size and spatial restriction of the motion.[13]

As for a given $\langle\log\tau_\beta\rangle$, the width of $G_\beta(\log\tau)$ does slightly vary among the systems,[14] $A(T)$ is not expected to be fully universal. Nevertheless the final state amplitude $1 - C^{cos}_{t_e}$ for t_e = 30 μs and 80 μs in toluene, ethanol,[13] CNCH and a mixture of chlorobenzene and decalin almost collapse on a single trend when plotted vs. $\log\tau_\beta$, cf. Figure 7(b). Included in the figure is the result of Eq. (20) calculated for the case of CNCH, whereby $p(t_e)$ serves as a fit parameter: the predicted evolution of $1 - C^{cos}_{t_e}$ in CNCH also closely mimics the experimental values of all other systems. The geometrical factor $f_G = p(80\ \mu s)/p(30\ \mu s)$, i.e., the evolution time dependence of $1 - C^{cos}_{t_e}$, was found to be ≈2.2 in all cases. Hence, ^{2}H NMR detects in all four systems a β-process with comparable degree of restriction that progresses via akin elementary steps, i.e., the mechanism of the motion appears universal, in particular, the relaxation strength in the investigated systems is virtually the same. We further emphasize that regarding ethanol, the β-process found in the glassy PC phase as well as in the structural glass ($T < T_g$) is virtually indistinguishable both in ^{2}H NMR[35] and DS[36] experiments.

The latter findings were already anticipated from the very similar t_p-dependent solid-echo line-shape observed in all systems below T_g (cf. Part I[15]). Consequently, the universality in mechanism is also expected to be found in the fast motion limit effects regarding the line-shape. As seen in Figure 8(a), the spectral width C_{80} collapses on a single trend (for $T < T_g$) when plotted vs. $\log\tau_\beta$ (the C_{80} values were normalized to coincide with respect to the lowest temperatures available for each system). The values only divert from a common behavior, when T_g of a system is surpassed (marked by the dotted lines, the T_g of toluene and chlorobenzene/decalin coincides) and hence the relaxation strength of the β-process grows. Consequently, the extension of the wobbling-in-a-cone model towards lower temperatures, as demonstrated in Figure 6, is fully valid also in case of the presented structural glass formers. The same holds for the spin-lattice relaxation time T_1, as demonstrated in Figure 8(b): on the $\log\tau_\beta$ scale, $\langle T_1\rangle$ almost collapses on a single trend for all systems (again for $T < T_g$ where 1-f is roughly constant). As the ^{2}H NMR coupling constants δ are of comparable magnitude among the samples, it directly follows according to Eq. (7), that also the spectral densities and hence $f^{(2)}$ have to be very similar. Once again we emphasize that type-A glass formers (without a β-process) show completely different $T_1(T)$ behavior.

In dielectric spectroscopy on the other hand, the situation is quite different: as demonstrated in Figure 8(c), 1-$f^{(1)}$ at $T < T_g$ varies by more than two orders of magnitude

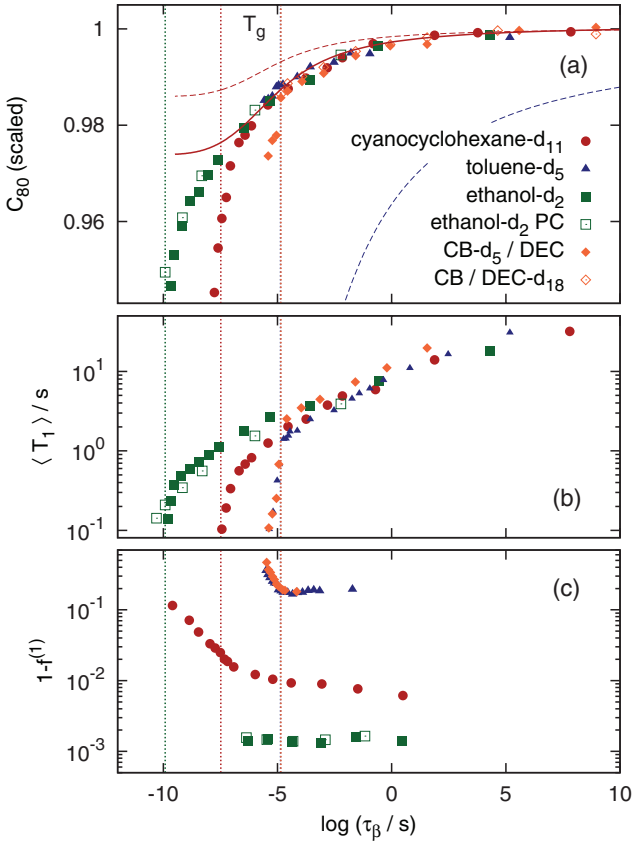

FIG. 8. (a) Normalized apparent spectral width C_{80} of CNCH, toluene, ethanol (glassy and PC phase)[37] and chlorobenzene/decalin on an isodynamic temperature scale with respect to the β-process, i.e., vs. $\log \tau_\beta$. The dotted lines in corresponding color mark the respective T_g, the dashed and full lines are calculated within the wobbling on a cone model for different opening angles χ, see text. X axis see (c). (b) Spin-lattice relaxation time $\langle T_1 \rangle$ of the same systems[13] on the same reduced temperature scale. (c) Dielectric relaxation strength $1 - f^{(1)} = \Delta\epsilon_\beta/\Delta\epsilon$ of the β-process for CNCH,[18] toluene,[7] ethanol,[36] and chlorobenzene/decalin[14] vs. $\log \tau_\beta$.

between toluene and ethanol. As the latter system represents a primary alcohol, $1\text{-}f^{(1)}$ may be underestimated due to the Debye peak, which interferes with the α-peak.[38] In the case of toluene, chlorobenzene/decalin and CNCH, however, the different manifestation of the β-process in DS is unambiguous (cf. Figure 9): $1\text{-}f^{(1)}$ below T_g differs by more than an order of magnitude, which is incompatible with our present NMR results. According to Eq. (17), a mean cone angle χ for the spatial restriction of the β-process can be obtained from $1\text{-}f^{(1)}$, which allows us to calculate the spectral width C_{80} via Eq. (15) (at $T < T_g$). As discussed above, the dielectric relaxation strength in CNCH is too small to reproduce our present NMR results: the dashed red curve in Figure 8(a) obtained from $1\text{-}f^{(1)}$ ($\chi^m = 8°$) clearly underestimates the universal line shape changes in all systems. In toluene on the other hand, the ample dielectric strength yields a mean cone opening angle of about 35° below T_g, which would induce pronounced line shape effects, as demonstrated by the dashed blue curve in Figure 8(a). Hence the dielectric relaxation strength, as given by $\Delta\epsilon_\beta/\Delta\epsilon$, of all presented glass forming systems is incompatible with our NMR results, which suggest a rather universal single-particle motion for the β-process.

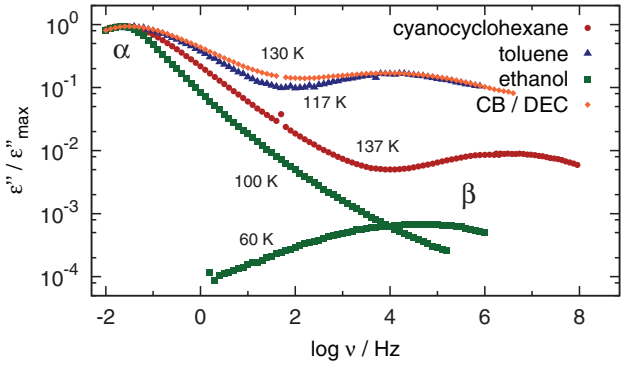

FIG. 9. Dielectric spectra of CNCH,[18] toluene,[7] ethanol,[36] and chlorobenzene/decalin[14] in the vicinity of T_g. For reasons of comparison the spectra are normalized with respect to the amplitude of the α-peak. Due to the fast β-process in ethanol, no dielectric spectrum covering α- and β-peak is available. The given low temperature spectrum (60 K) is normalized with respect to the α-peak at T_g.

III. DISCUSSION AND CONCLUSIONS

Due to the characteristics of the β-process in CNCH pronounced line-shape and T_1 effects were revealed in the ^{2}H NMR observables. Below T_g the mechanism of the β-process was shown to be virtually identical to the one observed in structural glass formers like toluene and ethanol as well as binary glasses, i.e., the secondary relaxation does not exhibit any peculiarities reflecting the translational order of the PC phase. Above T_g a pronounced minimum in T_1 is observed, in accordance with previous results in cyclohexanol.[26] T_1 was successfully modeled in the whole accessible temperature range by means of $\chi''_{\alpha/\beta}(\omega)$ from dielectric spectroscopy and a relaxation strength $1\text{-}f^{(2)}$ increasing with T. The striking similarities of T_1 in CNCH with respect to cyclohexanol (cf. Figure 2) suggest that the presented analysis also holds for the β-process in the latter compound.

Furthermore, the solid-echo line-shape shows strong and characteristic deviations from a Pake pattern in a large temperature range above T_g, a phenomenon not seen before in simple glass formers, reported however for polymers.[39] The spectra were successfully modeled via a motion restricted to a cone with a Gaussian distribution of opening angles $G(\chi; T)$. This approach directly arises from the behavior observed below T_g by a growing relaxation strength, i.e., via changes in the maximum and width of the distribution $G(\chi; T)$. Hence, the distribution of restricting geometries for the β-process, $G(\chi; T)$, was for the first time directly accessible to ^{2}H NMR via the fast motion limit line shape, which allowed for a confirmation of previously developed models for structural glass formers below T_g, where $G(\chi; T)$ cannot be quantified in straightforward manner.

The present study furthermore demonstrates the significance of the β-process for glassy dynamics via the ample growth in $1\text{-}f$ ($T > T_g$). This finding is in accordance with the random first-order transition theory of glasses, which predicts that the β-process becomes the dominant mode of structural relaxation at high temperatures,[40] and again raises questions with regard to the dynamics in structural glass formers at temperatures above the merging of α- and β-process.

Although we have demonstrated that ^{2}H NMR detects a β-process of universal single-particle dynamics in CNCH, toluene, ethanol, and mixtures of chlorobenzene with decalin, the dielectric relaxation strength varies strongly among the systems and is in neither case compatible with the NMR results. Whereas ^{2}H NMR measures a single particle correlation function, the differences in DS may arise from the fact that macroscopic fluctuations of the polarization are probed. Thus, the relaxation strength $\Delta\epsilon_\beta$ does not necessarily reflect a molecular property. For example, assume that some kind of assembly (including all molecules) of "clusters" is formed in which molecules move collectively. Then the effective dipole moment may be determined by the dipolar ordering within the cluster, i.e., does not reflect $1\text{-}f^{(1)}$ as introduced in modeling the process probed by ^{2}H NMR. Whereas the microscopic dynamics in terms of the single particle correlation function are elucidated in good approximation, the β-process retains some of its mystery with regard to the dielectric results and also the lack of a β-process in light scattering spectra[20,21] has to be further clarified. All this may be taken as a hint that the β-process is a cooperative process (as is the primary α-process).

ACKNOWLEDGMENTS

The financial support of the Deutsche Forschungsgemeinschaft through Project No. RO 907/10-1 is gratefully acknowledged.

[1] G. Johari and M. Goldstein, J. Chem. Phys. **53**, 2372 (1970).
[2] G. P. Johari, J. Chem. Phys. **58**, 1766 (1973).
[3] L. Wu, Phys. Rev. B **43**, 9906 (1991).
[4] A. Arbe, D. Richter, J. Colmenero, and B. Farago, Phys. Rev. E **54**, 3853 (1996).
[5] K. L. Ngai and M. Paluch, J. Chem. Phys. **120**, 857 (2004).
[6] G. Williams and D. C. Watts, Trans. Farad. Soc. **67**, 1971 (1971).
[7] A. Kudlik, C. Tschirwitz, S. Benkhof, T. Blochowicz, and E. Rössler, Europhys. Lett. **40**, 649 (1997).
[8] T. Blochowicz and E. A. Rössler, Phys. Rev. Lett. **92**, 225701 (2004).
[9] K. L. Ngai and S. Capaccioli, Phys. Rev. E **69**, 031501 (2004).
[10] C. Gainaru, R. Kahlau, E. A. Rössler, and R. Boehmer, J. Chem. Phys. **131**, 184510 (2009).
[11] M. Vogel and E. Rössler, J. Chem. Phys. **114**, 5802 (2001).
[12] M. Vogel and E. Rössler, J. Chem. Phys. **115**, 10883 (2001).
[13] M. Vogel, P. Medick, and E. A. Rössler, Annu. Rep. NMR Spectrosc. **56**, 231 (2005).
[14] M. Vogel, C. Tschirwitz, G. Schneider, C. Koplin, P. Medick, and E. Rössler, J. Non-Cryst. Solids **307–310**, 326 (2002).
[15] B. Micko, S. A. Lusceac, H. Zimmermann, and E. A. Rössler, J. Chem. Phys. **138**, 074503 (2013).
[16] S. Lusceac, I. Roggatz, P. Medick, J. Gmeiner, and E. A. Rössler, J. Chem. Phys. **121**, 4770 (2004).
[17] G. Hinze, Phys. Rev. E **57**, 2010 (1998).
[18] C. Tschirwitz, S. Benkhof, T. Blochowicz, and E. Rössler, J. Chem. Phys. **117**, 6281 (2002).
[19] L. Comez, D. Fioretto, L. Palmieri, L. Verdini, P. A. Rolla, J. Gapinski, T. Pakula, A. Patkowski, W. Steffen, and E. W. Fischer, Phys. Rev. E **60**, 3086 (1999).
[20] A. Brodin, R. Bergman, J. Mattsson, and E. A. Rössler, Eur. Phys. J. B **36**, 349 (2003).
[21] N. Petzold, B. Schmidtke, R. Kahlau, D. Bock, R. Meier, B. Micko, D. Kruk, and E. A. Rössler, J. Chem. Phys. **138**, 12A510 (2013).
[22] G. Lipari and A. Szabo, J. Am. Chem. Soc. **104**, 4546 (1982).
[23] T. Blochowicz, A. Kudlik, S. Benkhof, J. Senker, E. Rössler, and G. Hinze, J. Chem. Phys. **110**, 12011 (1999).
[24] C. J. F. Böttcher and P. Bordewijk, *Theory of Electric Polarization I: Dielectrics in Static Fields* (Elsevier, Amsterdam, 1978).
[25] D. Abragam, *Principles of Nuclear Magnetism* (Oxford University Press, Oxford, 1973).
[26] P. L. Kuhns and M. S. Conradi, J. Chem. Phys. **80**, 5851 (1984).
[27] D. A. Torchia and A. Szabo, J. Magn. Reson. **49**, 107 (1982).
[28] L. S. Lusceac, I. Roggatz, J. Gmeiner, and E. A. Rössler, J. Chem. Phys. **126**, 014701 (2007).
[29] E. Rössler, M. Taupitz, and H. M. Vieth, J. Phys. Chem. **94**, 6879 (1990).
[30] C. Gainaru, O. Lips, A. Troshagina, R. Kahlau, A. Brodin, F. Fujara, and E. A. Rössler, J. Chem. Phys. **128**, 174505 (2008).
[31] K. Kinosita, S. Kawato, and A. Ikegami, Biophys. J. **20**, 289 (1977).
[32] C. Wang and R. Pecora, J. Chem. Phys. **72**, 5333 (1980).
[33] A. E. Sitnitsky, J. Magn. Reson. **213**, 58 (2011).
[34] L. S. Batchelder, C. H. Niu, and D. A. Torchia, J. Am. Chem. Soc. **105**, 2228 (1983).
[35] G. Schneider, Master's thesis, Universität Bayreuth, 2001.
[36] S. Benkhof, A. Kudlik, T. Blochowicz, and E. Rössler, J. Phys.: Condens. Matter **10**, 8155 (1998).
[37] R. Böhmer, G. Diezemann, G. Hinze, and E. Rössler, Prog. Nucl. Magn. Reson. Spectrosc. **39**, 191 (2001).
[38] C. Gainaru, R. Meier, S. Schildmann, C. Lederle, W. Hiller, E. A. Rössler, and R. Böhmer, Phys. Rev. Lett. **105**, 258303 (2010).
[39] A. S. Kulik, H. W. Beckham, K. Schmidt-Rohr, D. Radloff, U. Pawelzik, C. Boeffel, and H. W. Spiess, Macromolecules **27**, 4746 (1994).
[40] J. D. Stevenson and P. G. Wolynes, Nat. Phys. **6**, 62 (2010).